KSME

Springer

Journal of Mechanical Science and Technology 36 (9) 2022

Original Article
DOI 10.1007/s12206-022-0818-y

Keywords:
· Creep
· Next-generation nuclear plants
· Modified 9Cr-1Mo steel
· Small punch test

Correspondence to:
Moon Ki Kim
mkkim1212@skku.edu

Citation:
Kim, S., Ro, U., Kim, Y. H., Lee, T., Kim, M. K. (2022). Evaluation of creep properties using small punch creep test for modified 9Cr-1Mo steel. Journal of Mechanical Science and Technology 36 (9) (2022) 4549~4561.
http://doi.org/10.1007/s12206-022-0818-y

Received November 19th, 2021
Revised May 2nd, 2022
Accepted May 16th, 2022

† Recommended by Editor Chongdu Cho



# Evaluation of creep properties using small punch creep test for modified 9Cr-1Mo steel

**Sangyeop Kim[1], Uijeong Ro[1], Yong Hwi Kim[1], Taeksang Lee[2] and Moon Ki Kim[1,3]**

[1]School of Mechanical Engineering, Sungkyunkwan University, 2066 Seobu-ro, Jangan-gu, Suwon-si, Gyeonggi-do, Korea, [2]Department of Mechanical Engineering, Myongji University, 116 Myongji-ro, Cheoin-gu, Yongin-si, Gyeonggi-do, Korea, [3]SKKU Advanced Institute of Nano Technology (SAINT), Sungkyunkwan University, 2066 Seobu-ro, Jangan-gu, Suwon-si, Gyeonggi-do, Korea

**Abstract** In the pressure vessel of a very-high-temperature reactor (VHTR), creep damage, which has a fatal adverse effect on safe operation, occurs due to long-term operation at a higher temperature. In this paper, only the small punch creep test (SPCT) was used to evaluate the creep properties of modified 9Cr-1Mo steel, which is considered a suitable candidate material for VHTR pressure vessels. Since the test outputs of SPCT are displacement and load, we converted those outputs into the strain and stress of conventional uniaxial creep tests (UCTs). The Norton, Larson-Miller and Monkman-Grant creep models were constructed using the conversion data from SPCT and the triangular relationship among the three creep models was successfully demonstrated. Finally, those three models were constructed using long-term UCT with the same material and temperature, and the validity of this study was verified by comparing it with SPCT results.

## 1. Introduction

Today, as technology advances and the number of people around the world increases, the demand for energy is rapidly increasing. According to a 2020 report published by the International Energy Agency (IEA), most energy is currently produced by fossil fuels such as coal, oil, and natural gas to meet global energy needs, accounting for about 81 % of global energy production in 2018 [1]. Fossil fuels are widely used today as the primary energy resource in various industries, transportation modes, and homes, thanks to their convenient transportability, storage, and excellent energy efficiency. However, the sources of fossil fuels are currently rapidly diminishing and the fuels themselves cause serious environmental pollution problems such as greenhouse gases, ozone hole generation, and production of acid rain. Due to such fatal disadvantages of fossil fuels, the development of sustainable and eco-friendly energy resources that can replace fossil fuels is a very important issue worldwide.

Nuclear energy is expected to be an alternative to fossil fuels as an eco-friendly energy resource while meeting the rapidly increasing energy demand around the world. According to a report published in 2019 by the International Atomic Energy Agency (IAEA), there were about 450 nuclear power plants in operation worldwide as of 2018, accounting for about 10 % of global energy production [2]. However, those plants need improvement or replacement to address the safety concerns of aging and to also take on a larger share of global energy production.

Accordingly, research on and development of the next-generation nuclear plant (NGNP), known as the generation-IV nuclear power reactor, is being carried out by the IAEA and the Organisation for Economic Co-operation and Development's Nuclear Energy Agency (OECD NEA) [3, 4]. There are currently six types of NGNPs: gas-cooled fast reactor (GFR), lead-cooled reactor (LFR), molten salt reactor (MSR), sodium-cooled fast reactor (SFR), very-high-temperature reactor (VHTR), and super-critical water-cooled reactor (SCWR), according to the

neutron energy spectrum. Among them, the VHTR is currently being developed with the highest priority as it is considered to be closest to utilization [3-5]. The VHTR is designed to operate at higher temperatures than currently-operating nuclear power plants to increase its energy efficiency and have a longer service life (60 years or more) [5]. However, due to operating conditions in which components are exposed to a high-temperature environment for a long time, creep damage that occurs in the pressure vessel of a VHTR can adversely affect its stable operation.

Creep damage occurs when a metallic material is exposed to a high-temperature environment where stress occurs for a long time. Damage accumulates internally even though the stress applied to the metallic material is less than the yield stress, resulting in deformation and cracking over time. Therefore, creep damage is considered very important in evaluating the integrity of facilities exposed to high-temperature environments where stress occurs for a long time. Many researchers have studied creep property evaluation methods for metallic materials. In general, such evaluations are conducted through the uniaxial creep test (UCT) proposed in ASTM E139-11 [6]. The UCT is a test method for evaluating creep properties over time by applying a constant load below the yield stress of the metallic material at both ends of the uniaxial test specimen in a high-temperature environment, resulting in strain over time at specific temperature and stress conditions. The UCT has the advantage of being able to immediately assess the integrity of various facilities, as the strain and stress values are directly derived from the test results. However, there is a fundamental limitation that the test process consumes a substantial amount of materials and takes a long time to produce results. Therefore, the UCT has a disadvantage in that it cannot evaluate real-time properties reflecting the operating history of facilities in operation.

As an alternative to overcome these fundamental limitations of the UCT method, a method for evaluating the properties of metallic materials using small specimens was proposed in the 1980s [7, 8]. Initially, this small punch test method was developed to evaluate the post-irradiation effects in nuclear power plants [7, 8], and was then expanded to evaluating the straightforward properties of metallic materials such as tensile strength [9, 10] and creep deformation [11]. The small punch creep test (SPCT) utilizes very thin specimens to evaluate the creep properties of metallic materials, and is largely composed of four elements: the metallic specimen which is 1/200 in volumetric size compared to that needed for the UCT; a punch ball that directly contacts the specimen and applies a constant supplied load to it; a punch that delivers a constant load generated from the testing machine to the punch ball; and an upper and lower die for fixing the specimen. Because SPCT uses much smaller specimens compared to UCT, it has the advantage that very little material is consumed and it takes relatively little time to obtain test results. Thanks to these advantages, with SPCT it is possible to evaluate real-time material properties that reflect the operating history of facilities.

However, unlike UCT, wherein strain and stress data are derived from the test results, SPCT derives displacement and load data from the test results, making it difficult to directly apply SPCT to evaluate the integrity of a facility. In order to utilize SPCT for integrity evaluation, it is essential to establish the correlation between the strain and stress of UCT and the displacement and load of SPCT. However, because SPCT specimens are in a multi-axial stress state, this correlation is a very complicated process. To date, several researchers have used various means to establish the correlation(s) between UCT and SPCT test result data [12-20]. Among these studies, based on Chakrabarty's membrane stretching theory [21], Lee et al. [19] proposed a methodology for converting the displacement of SPCT into the strain of UCT, and Kim et al. [20] proposed a methodology for converting the load of SPCT into the stress of UCT.

Therefore, the main objective of this paper is to evaluate creep properties of modified 9Cr-1Mo steel, which is a candidate material for VHTR pressure vessels, using only SPCT. First, SPCT was carried out at 550 °C, the target operating temperature of a given VHTR. Then the displacement data of SPCT was converted into the strain data of UCT using the methodology proposed by Lee et al. [19], and the load data of SPCT was converted into the stress data of UCT using the methodology proposed by Kim et al. [20]. Based on these converted data, and following the approaches of Norton [22], Larson-Miller [23], and Monkman-Grant [24], creep property evaluation models using only SPCT for modified 9Cr-1Mo steel at a temperature 550 °C were constructed and a triangular relationship among the creep property evaluation models was successfully demonstrated. Finally, those creep property evaluation models were reconstructed using long-term UCT data at the same material and temperature provided by the (Japan) National Institute for Materials Science (NIMS) [25]. The validity of this study was verified by comparing the results with the creep property evaluation models constructed through the SPCT data.

## 2. Methods

### 2.1 Equivalent strain formulation

Lee et al. [19] proposed an equivalent strain formulation that converts the displacement of SPCT into the strain of UCT. In this study, based on Chakrabarty's membrane stretching theory [21], the equivalent strain, $\varepsilon_{eq}$, can be expressed in the following form:

$$\varepsilon_{eq} = \sqrt{\frac{2}{3}\varepsilon_{ij}^{'} : \varepsilon_{ij}^{'}} = \sqrt{\frac{2}{3}\varepsilon_{ij} : \varepsilon_{ij}} = \sqrt{\frac{2}{3}\left(\varepsilon_{\theta}^{\,2} + \varepsilon_{\varphi}^{\,2} + \varepsilon_{T}^{\,2}\right)} = \left|\varepsilon_{T}\right| = \ln\left(\frac{T_0}{T}\right) \tag{1}$$

where $\varepsilon_{ij}^{'}$ is the deviatoric strain tensor, $\varepsilon_{ij}$ is the plastic strain tensor, $\varepsilon_{\theta}$ is the circumferential strain, $\varepsilon_{\varphi}$ is the merid-

ional strain, $\varepsilon_T$ is the radial strain, which is in the direction of thickness, $T$ is the thickness of the specimen, and $T_0$ is the initial thickness of the specimen. Next, based on Mao's empirical equation [26], the thickness of the specimen at the specific punch displacement, $T(h)$, is defined as:

$$T(h) = T_0 e^{-1.2\left(\frac{h}{2}\right)^{1.5}} \tag{2}$$

where $h$ is the punch displacement. Finally, by substituting Eq. (2), which defines the thickness of the specimen at a specific punch displacement, into Eq. (1), the equivalent strain is expressed in the following form:

$$\varepsilon_{eq} = 1.2\left(\frac{h}{2}\right)^{1.5} \tag{3}$$

where $h$ is the punch displacement. Through Eq. (3), the equivalent strain formulation proposed by Lee et al., the strain data of UCT required for creep properties evaluation can be successfully obtained through only the punch displacement of SPCT.

## 2.2 Equivalent stress formulation

Kim et al. [20] proposed an equivalent stress formulation that converts the load of SPCT into the stress of UCT. In this study, based on Chakrabarty's membrane stretching theory [21], the equivalent stress, $\sigma_{eq}$, can be expressed in the following form:

$$\begin{aligned}\sigma_{eq} &= \sqrt{\frac{3}{2} S_{ij} : S_{ij}} = \sqrt{\frac{1}{2}\left(2\sigma_\theta^2 + 2\sigma_\varphi^2 - 2\sigma_\theta\sigma_\varphi\right)} \\ &= \left|\sigma_\theta\right| = \frac{F}{2\pi R T \sin^2\varphi}\end{aligned} \tag{4}$$

where $S_{ij}$ is the deviatoric stress tensor, $\sigma_\theta$ is the circumferential stress, $\sigma_\varphi$ is the meridional stress, $F$ is the load of SPCT, $R$ is the punch ball radius, and $T$ is the thickness of the specimen. Unlike the equivalent strain formulation, which only considers the thickness of the specimen, in the equivalent stress formulation both the thickness of the specimen and the contact angle between the specimen and the punch ball should be considered. Therefore, based on Chakrabarty's membrane stretching theory [21], the punch displacement at a specific contact angle, $h(\varphi)$, can be expressed in the following form:

$$h(\varphi) = R\sin^2\varphi \ln\left\{\frac{2\sin^2\frac{\varphi}{2}}{\sin^3\varphi}\left(\frac{a}{R} + \sqrt{\frac{a^2}{R^2} - \sin^4\varphi}\right)\right\} + 2R\sin^2\frac{\varphi}{2} \tag{5}$$

where $\varphi$ is the contact angle between the specimen and the punch ball and $a$ is the inner radius of the lower die. Since the equivalent stress in Eq. (4) uses the contact angle as a variable, the contact angle, which is the inverse form of Eq. (5), should be derived as a function of the punch displacement. It is very difficult to directly derive the inverse form due to the complexity of Eq. (5). So, by applying non-linear fitting, an approximation of the inverse form is expressed in the following form:

$$\varphi(h) = \ln(1 + 1.3h) \tag{6}$$

where $h$ is the punch displacement. Finally, by substituting Eq. (2) expressing the thickness of the specimen using Mao's empirical equation, and Eq. (6) expressing the contact angle using Charkrabarty's membrane stretching theory, into Eq. (4), the equivalent stress is expressed in the following form:

$$\sigma_{eq} = \frac{F}{2\pi R T_0 e^{-1.2\left(\frac{h}{2}\right)^{1.5}} \sin^2\left\{\ln(1+1.3h)\right\}} \tag{7}$$

where $F$ is the load of SPCT.

Eq. (7) expressing the equivalent stress was derived under the assumption that there was no frictional force between the specimen and the punch ball. However, in actual SPCT it is known that the frictional force between the specimen and the punch ball significantly affects the test results. Specifically, a study on the effect of frictional force between the specimen and the punch ball on small punch creep behavior conducted by Kim et al. [27] showed that the minimum punch displacement rate decreased as the frictional force increased and thus the failure time increased. Therefore, in order to increase the accuracy of the equivalent stress formulation, the frictional effect must be included. In this study, the stress distribution and the contact area variation are investigated at five types of friction coefficients ($\mu$ = 0, 0.2, 0.4, 0.6, 0.8) for contact between the specimen and the punch ball through finite element analysis (FEA). From these results, the frictional effect was simulated through a non-dimensional correction factor, $\alpha(\mu)$, which is expressed in the following form:

$$\alpha(\mu) = 0.95e^{-0.5\mu} \tag{8}$$

where $\mu$ is the friction coefficient. Finally, by multiplying the non-dimensional correction factor that simulates the frictional effect expressed in Eq. (8) and the equivalent stress formulation without the frictional effect expressed in Eq. (7), the equivalent stress, $\sigma_{eq}^{'}$, including the frictional effect, is expressed in the following form:

$$\sigma_{eq}^{'} = \alpha(\mu) \times \sigma_{eq} = \left(0.95e^{-0.5\mu}\right) \times \sigma_{eq} \tag{9}$$

where $\mu$ is the friction coefficient. Through Eq. (9), the equivalent stress formulation proposed by Kim et al., the stress data of UCT required for creep properties evaluation can be successfully obtained through the punch displacement and

load of SPCT.

### 2.3 Creep property evaluation models

The Norton model [22] is used to evaluate the creep properties of metallic materials utilizing the minimum strain rate, $\dot{\varepsilon}_{min}$, and stress, $\sigma$, and is expressed in the following form:

$$\dot{\varepsilon}_{min} = A_N \sigma^n \tag{10}$$

where $A_N$ and $n$ are temperature-dependent material properties. The secondary creep stage, known as steady-state creep, accounts for most of the total creep life and has a constant and minimum strain rate due to the balance between strain hardening and thermal softening. Therefore, this model can evaluate the overall creep properties by evaluating the minimum strain rate at each stress condition. Also, this model is usually used to evaluate the creep properties after conversion to logarithmic scale:

$$\log \dot{\varepsilon}_{min} = n \log \sigma + \log A_N . \tag{11}$$

After conversion to logarithmic scale as in Eq. (11), $\log \dot{\varepsilon}_{min}$ and $\log \sigma$ have a linear relationship with a slope of $n$. Finally, we can evaluate the properties of long-term creep by constructing the Norton model through short-term creep tests and then performing linear approximation to the linear relationship in the logarithmic scale.

The Larson-Miller model [23] based on the Arrhenius equation is usually used to evaluate the effect of stress and temperature on the creep life of metallic materials. Assuming that the activation energy is a function of stress, the Larson-Miller parameter is expressed in the following form:

$$LMP = T\left(C_{LM} + \log t_f\right) \tag{12}$$

where $LMP$ is the Larson-Miller parameter, $T$ is the absolute temperature, $C_{LM}$ is a material constant that usually has a value of 20 (but varies from 10 to 40 depending on the material), and $t_f$ is the creep life. This model evaluates the creep properties of metallic materials through the characteristic that $LMP$ (including temperature and creep life) and stress have a linear relationship. This linear relationship is expressed in the following form:

$$\sigma = A_{LM} * LMP + B_{LM} \tag{13}$$

where $A_{LM}$ and $B_{LM}$ are the material constants. Finally, we can successfully predict the long-term creep life of metallic materials as a function of temperature and stress by constructing the Larson-Miller model using the short-term creep life measured at high stress.

The Monkman-Grant model [24] is used to predict the creep life, $t_f$, as a function of the minimum strain rate, $\dot{\varepsilon}_{min}$, for metallic materials, and is expressed in the following form:

$$t_f \dot{\varepsilon}_{min}{}^m = C_{MG} \tag{14}$$

where $m$ and $C_{MG}$ are the material constants that depend on the temperature. In general, the material constant $m$ has a value between 0.8 and 0.95 and $C_{MG}$ has a value between 3 and 20. This model is usually used to evaluate creep properties after conversion to logarithmic scale:

$$\log t_f = -m \log \dot{\varepsilon}_{min} + \log C_{MG} . \tag{15}$$

After conversion to logarithmic scale as in Eq. (15), $\log t_f$ and $\log \dot{\varepsilon}_{min}$ have a linear relationship with a slope of $-m$. Finally, we can predict long-term creep life by constructing the Monkman-Grant model through short-term creep tests and then performing a linear approximation of the linear relationship in the logarithmic scale.

### 2.4 Triangular relationship among the creep property evaluation models

As mentioned earlier, the Norton, Larson-Miller, and Monkman-Grant models are used to evaluate the creep properties of metallic materials. The Norton model consists of minimum strain rate and stress, the Larson-Miller model consists of stress and creep life, and the Monkman-Grant model consists of creep life and minimum strain rate. Therefore, the Norton and Larson-Miller models have stress, the Larson-Miller and Monkman-Grant models have creep life, and the Monkman-Grant and Norton models have minimum strain rate as a common variable. Given the fact that binary sets of these models share common variables, these three creep property evaluation models can be said to constitute a triangular relationship. Specifically, the remaining models can be obtained by redefining the two types of models among the three types of creep property evaluation models with respect to common variables. For example, the common variable of the Norton and Larson-Miller models is stress, and these two models can be redefined for that common variable. Then, based on the two redefined models for stress, the Monkman-Grant model can be derived.

## 3. Experimental

### 3.1 Material

In this study, modified 9Cr-1Mo steel was the SPCT specimen. As mentioned earlier, since NGNPs are expected to operate for a longer time under elevated operating conditions compared to previous-generation nuclear power plants, creep damage that has a fatal adverse effect on plant safety occurs. Therefore, modified 9Cr-1Mo steel, which shows excellent resistance to creep damage at high temperatures, is being considered as a candidate material for the pressure vessels of

VHTRs, which are being developed as the top priority among NGNPs. The specific chemical composition and mechanical properties of the modified 9Cr-1Mo steel are shown in Tables 1 [28] and 2 [29], respectively.

### 3.2 SPCT procedure

SPCT is a test method to evaluate the creep properties of metallic materials by measuring the punch displacement over time by applying constant load to very thin specimen sheets with a punch ball. Here, SPCT was carried out at 550 °C, the target operating temperature of VHTR pressure vessels. The spherical punch ball was made of $Si_3N_4$ with a radius of 1.2 mm, and the specimen sheet was 10×10 with a thickness of 0.5 mm, as shown in Fig. 1(a). Because SPCT specimens are necessarily much thinner than UCT specimens, foreign substances such as oxides generated on the surface of the specimen during processing and storage can significantly undermine the reliability of the SPCT results. Therefore, the original specimen size of 10×10 with a thickness of 0.6 mm was polished to a thickness of 0.5 mm to remove all foreign substances. Additionally, as shown in Fig. 1(b), slippage between the specimen and the punch ball was prevented by securely installing the specimen between the upper and lower dies of the jig, and the load generated from the test device was transferred to the specimen through the punch and the punch ball. The punch and upper and lower dies were made of Inconel alloy 617 which has high strength, oxidation resistance and corrosion resistance even at temperatures above 980 °C to secure the reliability and stability of SPCT.

We carried out the SPCT at high temperature using the test machine as shown in Fig. 2(a), which consisted of a gas flow controller, a loading frame, and a chiller. The chamber of the loading frame is a cylindrical shape with a radius of 150 mm and a height of 200 mm, and is made of SUS304 to perform SPCT stably at high temperatures. Also, the design pressure is 10 bar, the heating element is Kanthal A1, the heating power is 220 V, 1 Ph, 3 kW, and the maximum operating temperature is 1000 °C. The jig holding the specimen was placed inside the chamber of the loading frame, as shown in Fig. 2(b). The temperature of the specimen is measured by directly contacting the specimen with a type K thermocouple attached to the inside of the chamber. Because SPCT is carried out at high temperatures (~550 °C), high-temperature oxidation and overheating problems in the chamber during the test can prevent stable test progress. Therefore, prior to the test, the rotary pump was operated through the control panel of the gas flow controller to establish a near-vacuum inside the chamber. Inert argon gas

Table 1. Chemical composition of modified 9Cr-1Mo steel [28].

| Element | Nominal |
|---|---|
| Cr | 8.00-9.50 |
| Mo | 0.85-1.05 |
| V | 0.18-0.25 |
| Nb | 0.06-0.10 |
| C | 0.08-0.12 |
| Mn | 0.30-0.60 |
| Cu | 0.40 (max.) |
| Si | 0.20-0.50 |
| N | 0.03-0.07 |
| Ni | 0.40 (max.) |
| P | 0.02 (max.) |
| S | 0.01 (max.) |
| Ti | 0.01 (max.) |
| Al | 0.02 (max.) |
| Zr | 0.01 (max.) |
| Fe | Balance |

Table 2. Mechanical properties of modified 9Cr-1Mo steel at 550 °C [29].

| Mechanical property | Value |
|---|---|
| YS (MPa) | 336 |
| UTS (MPa) | 375 |
| E (GPa) | 125 |
| EL (%) | 25 |
| RA (%) | 91 |
| Strength coefficient (MPa) | 671 |
| Strain hardening exponent | 0.12 |

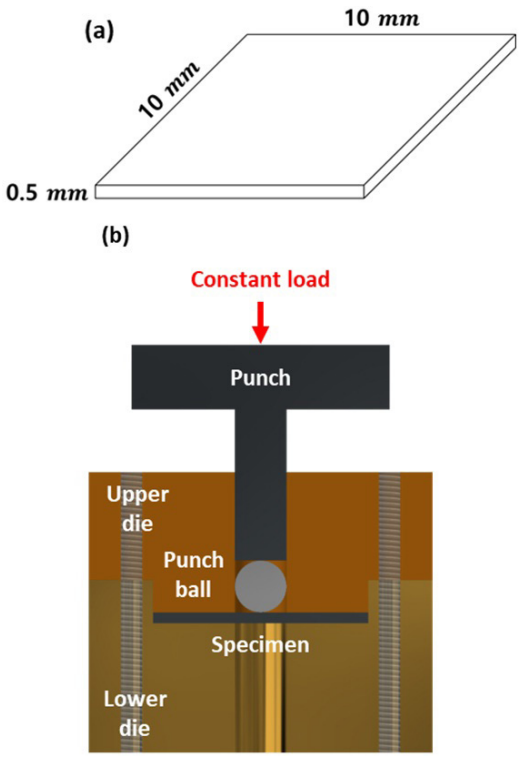


Fig. 1. Schematics of small punch creep test: (a) specimen; (b) jig.

was injected to create an appropriate gas atmosphere during the test, and cooling water was supplied through the chiller to prevent overheating inside the chamber. Then the target test temperature was set through the temperature indicator of the gas flow controller, and the temperature of the specimen was slowly increased over about 3 hours through the thermocouple inside the chamber.

After completing all these preparations, a load cell consisting of a servo motor that could impose a maximum load of 200 kgf on the loading frame, and a velocity reducer of 1:30, applied a constant load to the specimen by pushing the load into the chamber. The specimen delivering a constant load through the punch ball is stretched to cover the open bottom of the jig, and the punch displacement is derived over time as the output of the test. This punch displacement was measured with high precision using a 12-mm length gauge in the loading frame and a linear variable displacement transducer (LVDT) with 0.005-μm resolution.

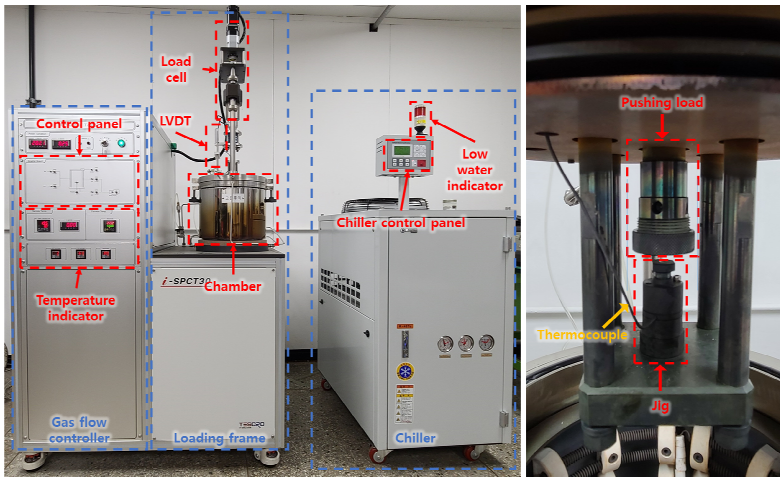


(a) (b)

Fig. 2. Small punch creep test machine: (a) gas flow controller, loading frame, and chiller; (b) inside the chamber.

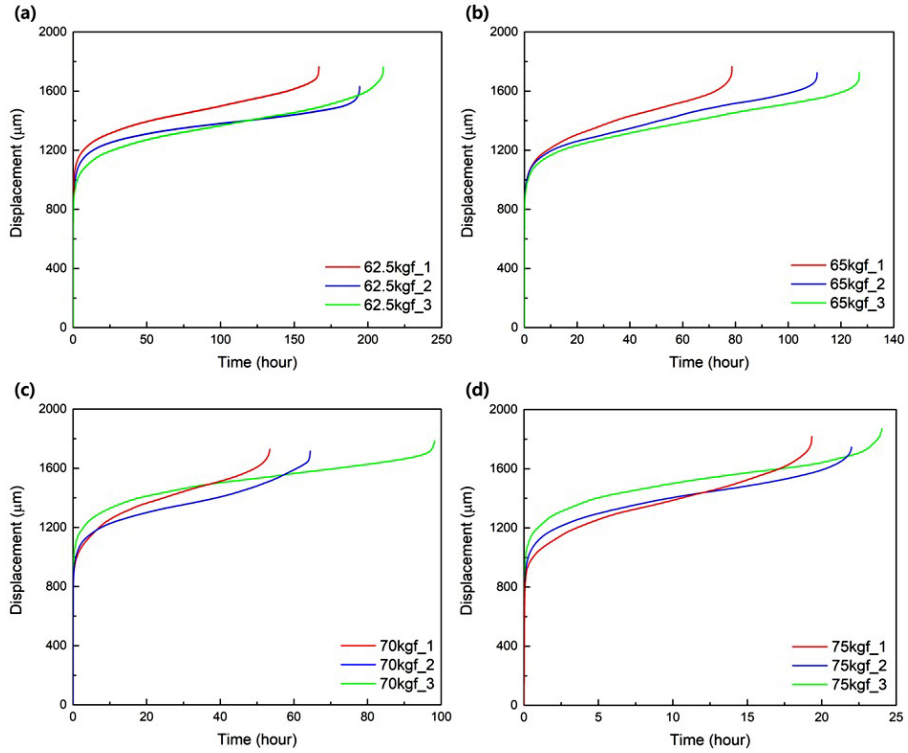


Fig. 3. Small punch creep test curves of modified 9Cr-1Mo steel at 550 °C: (a) 62.5 kgf; (b) 65 kgf; (c) 70 kgf; (d) 75 kgf.

## 4. Results and discussion

### 4.1 SPCT for modified 9Cr-1Mo steel

SPCT was performed on modified 9Cr-1Mo steel at the high temperature of 550 °C under a total of four different loading conditions: 62.5 kgf, 65 kgf, 70 kgf, and 75 kgf. In order to secure the reliability of the test results, it was repeated three times under each loading condition. Fig. 3 shows the punch displacement curve over time, which resembles the UCT strain curve over time. In general terms, the strain vs. time graph consists of four stages: the instantaneous deformation stage in which the strain rapidly increases at a constant rate at the beginning of the test; the primary creep stage in which the strain rate decreases and the creep resistance increases due to the self-strain of the material; the secondary creep stage in which the strain rate is constant and most of the creep life is covered due to the balance between the strain hardening and recovery; and the tertiary creep stage in which the strain rate rapidly increases, the cross-sectional area is reduced, and the material is broken due to the occurrence of necking. From Fig. 3, the tendency of the displacement change in SPCT is very similar to that of the strain change in each stage of UCT. The failure times measured under each loading condition can be confirmed in detail in Table 3: the average failure times were 190.52 hour, 105.51 hour, 72.02 hour, and 21.79 hour under each loading condition. The next section describes our analysis to convert the punch displacement and load output of SPCT into the strain and stress of UCT, in order to directly utilize SPCT to evaluate the creep properties of metallic materials.

Table 3. Small punch creep test results of modified 9Cr-1Mo steel at 550 °C.

| Load (kgf) | Failure time (hour) |
|---|---|
| 62.5 | 166.79 |
| | 194.44 |
| | 210.34 |
| 65 | 78.68 |
| | 110.93 |
| | 126.91 |
| 70 | 53.46 |
| | 64.42 |
| | 98.18 |
| 75 | 19.34 |
| | 22.00 |
| | 24.04 |

### 4.2 Equivalent strain & stress analysis

Using Eq. (3), the equivalent strain formulation proposed by Lee et al. [19], the punch displacement of SPCT was converted

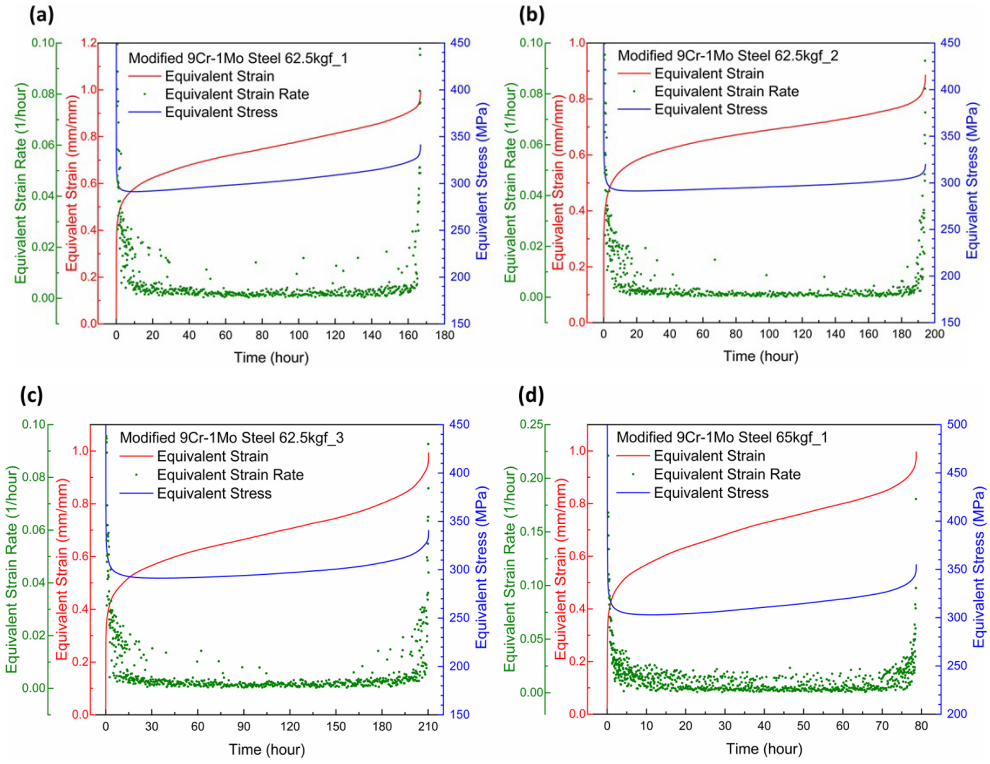


Fig. 4. Equivalent strain, strain rate, and stress curves of modified 9Cr-1Mo steel at 550 °C: (a)-(c) 62.5 kgf; (d)-(f) 65 kgf; (g)-(i) 70 kgf; (j)-(l) 75 kgf (continued).

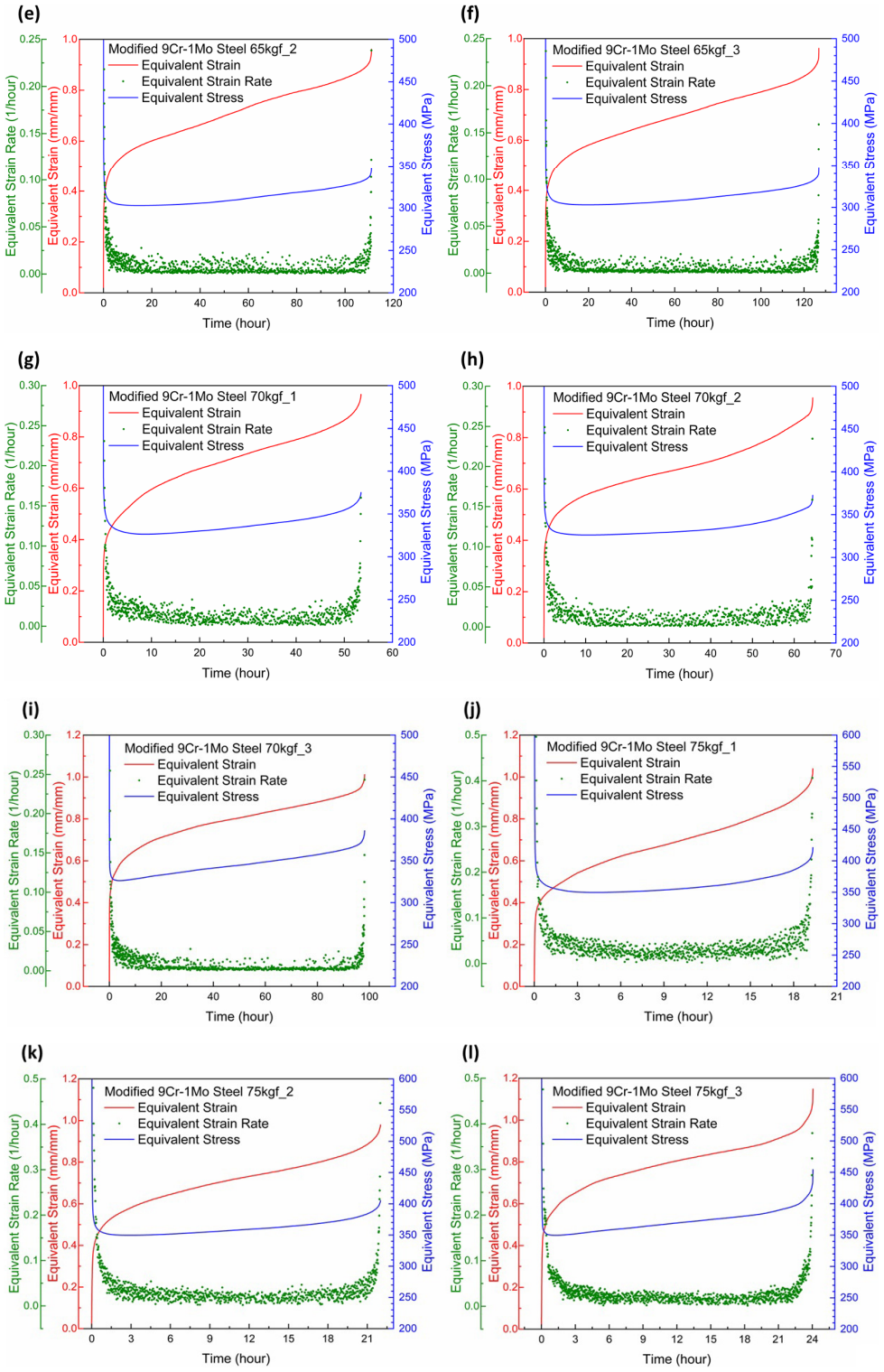


Fig. 4. (Continued).

into the strain of UCT; the resulting equivalent strain is expressed as curve as shown in Fig. 4. Like the strain curve of UCT, this equivalent strain curve consists of four stages: the instantaneous deformation, primary creep, secondary creep, and tertiary creep stages. The Norton and Monkman-Grant models use the minimum strain rate, not the strain, to evaluate the creep properties of metallic materials, so an additional process of selecting the minimum strain rate from the equivalent strain curve is required. Therefore, the equivalent strain rate is expressed as shown in Fig. 4 by differentiating each

equivalent strain point. As mentioned earlier, the creep strain rate at the secondary creep stage, which accounts for most of the creep life, is minimal and constant, whereas there is considerable noise in the equivalent strain rate values because an excessive amount of data is generated in the creep test over a long period of time. To solve this noise problem, the average value of the equivalent strain rate in the range of 30 %-70 % based on the creep life was selected as the representative minimum equivalent strain rate.

Next, using the equivalent stress formulation proposed by Kim et al. [20], the load of SPCT was converted into the stress of UCT. The equivalent stress was derived by applying the load and punch displacement data of SPCT to Eq. (7). However, since the previously derived equivalent stress did not include the frictional effect between the punch ball and the specimen, a non-dimensional correction factor, $\alpha(\mu)$ that included the friction coefficient $\mu$, as in Eq. (8), was introduced to derive the equivalent stress including the frictional effect. Jeong et al. [30] conducted a study on SPCT behaviors with various friction coefficients using the elastoplastic finite element method (FEM). That study found that the friction coefficient value that adequately simulates the actual SPCT behaviors of the modified 9Cr-1Mo steel is 0.7. Therefore, we derived the equivalent stress (including the frictional effect) by applying the equivalent stress without the frictional effect and 0.7, the friction coefficient value of the modified 9Cr-1Mo steel, to Eq. (9); the equivalent stress is expressed as a curve as shown in Fig. 4.

UCT has a constant stress value for the entire time that the stress is applied because the specimen is in a uniaxial stress state. However, unlike UCT, the SPCT equivalent stress value rapidly decreases at the beginning of the stress application and rapidly increases just before the specimen fractures because the specimen is in a multi-axial stress state. Since the Norton and Larson-Miller models use stress to evaluate the creep properties of metallic materials, it is essential to select a representative value among the changing equivalent stress values. Therefore, based on the creep life we selected the average value of the equivalent stress in the region of 30 %-70 % as the representative equivalent stress.

Finally, the values of the representative equivalent minimum strain rate and representative equivalent stress derived only through SPCT for each loading condition are shown in Table 4. The representative equivalent minimum strain rate and representative equivalent stress were consistently derived at each loading condition, and the minimum strain rate increased as the stress increased. This means that the SPCT showed that the creep life of the metallic material was shortened, as shown with the conventional creep test method UCT.

Table 4. Equivalent strain and stress analysis results of modified 9Cr-1Mo steel at 550 °C.

| Load (kgf) | Number | Representative minimum equivalent strain rate (1/hour) | Representative equivalent stress (MPa) |
|---|---|---|---|
| 62.5 | 1 | 0.002171 | 301.7 |
| | 2 | 0.001462 | 295.5 |
| | 3 | 0.001784 | 295.6 |
| 65 | 1 | 0.006908 | 310.4 |
| | 2 | 0.006043 | 310.1 |
| | 3 | 0.004634 | 308.8 |
| 70 | 1 | 0.010069 | 333.4 |
| | 2 | 0.008494 | 330.6 |
| | 3 | 0.004062 | 344.2 |
| 75 | 1 | 0.02492 | 355.2 |
| | 2 | 0.01967 | 357.6 |
| | 3 | 0.01740 | 369.0 |

## 4.3 Creep property evaluation models through SPCT

The Norton, Larson-Miller and Monkman-Grant creep property evaluation models were constructed using the equivalent minimum strain rate and equivalent stress derived only through SPCT. Thereafter, the validity of these models was verified by establishing a triangular relationship among the three models.

First, the Norton was constructed using the equivalent minimum strain rate data at each equivalent stress derived through SPCT. After plotting the equivalent minimum strain rate and equivalent stress, the Norton model expressed as Eq. (10) was constructed by performing non-linear fitting. Next, the Larson-Miller model was constructed using the rupture time data at each equivalent stress derived through SPCT. This model does not directly utilize the rupture time to evaluate the creep properties, but simultaneously evaluates the effect of temperature on the failure time of metallic materials by converting the rupture time into $LMP$ expressed as Eq. (12). The material constant, $C_{LM}$, included in the $LMP$ generally has a value of 20, but can vary between 10 and 40 depending on the material type. Therefore, in order to accurately construct the Larson-Miller model it is essential to use the $C_{LM}$ value appropriate for the target material. Through probabilistic and statistical analysis of the creep rupture data of modified 9Cr-1Mo steel, Choudhary et al. [31] proposed 35 as the $C_{LM}$ value for that material. Therefore, using 35 as the value of $C_{LM}$, we calculated the $LMP$ value of each failure time at the temperature of 550 °C. After plotting the equivalent stress and $LMP$, linear fitting was performed to construct the Larson-Miller model expressed as Eq. (13). Finally, the Monkman-Grant model was constructed using the failure time and minimum strain rate data derived through SPCT. After plotting the failure time and equivalent minimum strain rate, non-linear fitting was performed to construct the Monkman-Grant model expressed as Eq. (14).

Next, a triangular relationship was established among the three creep property evaluation models constructed through SPCT data. As mentioned earlier, the Norton and Larson-Miller models have stress as a common variable, Larson-Miller and Monkman-Grant models have creep life, and Monkman-Grant and Norton models have minimum strain rate. Through a trian-

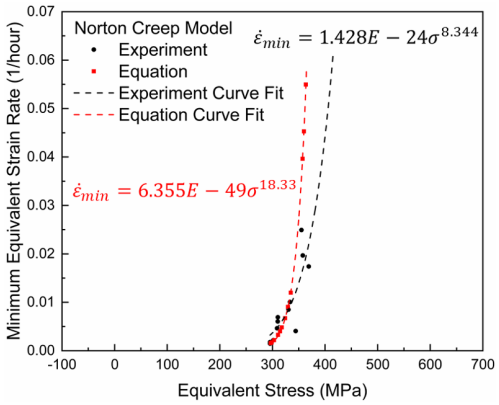


(a)

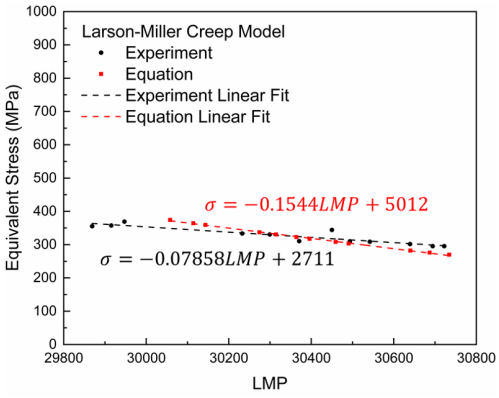


(b)

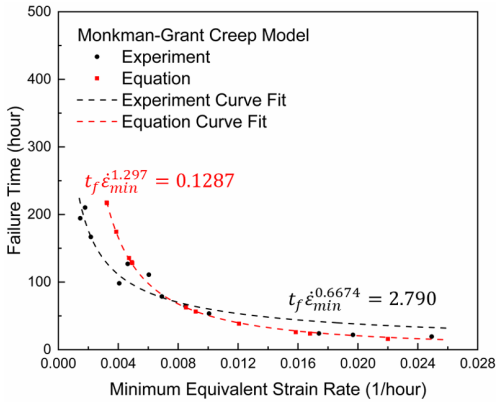


(c)

Fig. 5. Creep properties evaluation models of modified 9Cr-1Mo steel for comparison between experiment and equation: (a) Norton; (b) Larson-Miller; (c) Monkman-Grant.

gular relationship with the common variables in these binary sets, the final model was constructed by redefining each set of two models with respect to their common variable.

Finally, the three creep property evaluation models constructed through SPCT are expressed as 'experiment' in Fig. 5, and the models constructed considering a triangular relationship of these models are expressed as 'equation' in Fig. 5. The specific material constants of each model are shown in Table 5. The creep property evaluation models constructed through SPCT and the triangular relationship show quite similar results. This demonstrates that appropriate creep property evaluation models can be constructed using only SPCT.

Table 5. Material constants of modified 9Cr-1Mo steel at 550 °C for comparison between experiment and equation.

| Creep model | Material constant | Experiment | Equation |
|---|---|---|---|
| Norton creep model $\dot{\varepsilon}_{min} = A_N\sigma^n$ | $A_N$ | 1.428E-24 | 6.355E-49 |
| | $n$ | 8.344 | 18.33 |
| Larson-Miller creep model $\sigma = A_{LM} * LMP + B_{LM}$ | $A_{LM}$ | -0.07858 | -0.1544 |
| | $B_{LM}$ | 2711 | 5012 |
| Monkman-Grant creep model $t_f\dot{\varepsilon}_{min}^m = C_{MG}$ | $m$ | 0.6674 | 1.297 |
| | $C_{MG}$ | 2.790 | 0.1287 |

## 4.4 Creep property evaluation models through UCT

NIMS [25] performed long-term UCT on modified 9Cr-1Mo steel under various stress conditions with fracture times between 200 and 50000 hours at 550 °C, and provided the failure time and minimum strain rate data for each stress condition derived from those results. We constructed Norton, Larson-Miller, and Monkman-Grant creep property evaluation models using the data derived through UCT, and verified the validity of the data derived through SPCT by comparing it with models constructed through UCT.

First, the Norton model was constructed using the minimum strain rate data at each stress measured by UCT. Since the range of the minimum strain rate measured by UCT was much wider than that of SPCT, the Norton model expressed as Eq. (11) was constructed by converting the stress and minimum strain rate to logarithmic scale and then performing linear fitting. Next, the Larson-Miller model was constructed using the failure time data at each load measured by UCT. In the same manner as we previously calculated $LMP$ through SPCT, the $LMP$ value of each failure time at the temperature of 550 °C was calculated, using 35 as the $C_{LM}$ value for the modified 9Cr-1Mo steel. Then the material constants of the Larson-Miller model expressed as Eq. (13) were calculated through linear fitting between stress and $LMP$. Finally, the Monkman-Grant model was constructed using the failure time and minimum strain rate data measured through UCT. Since the range of the failure time and minimum strain rate measured by UCT was much wider than that of SPCT, the Monkman-Grant model expressed as Eq. (15) was constructed by converting the failure time and minimum strain rate to logarithmic scale and then performing linear fitting.

The three creep property evaluation models constructed with UCT and SPCT are shown in Fig. 6 and the specific material constants of each model are shown in Table 6. Tables 5 and 6 show the material constants of the creep property evaluation models constructed from the same SPCT data; in both cases the Larson-Miller model was constructed by directly applying

Table 6. Material constants of modified 9Cr-1Mo steel at 550 °C for comparison between uniaxial and small punch creep test.

| Creep model | Material constant | UCT | SPCT |
|---|---|---|---|
| Norton creep model $\dot{\varepsilon}_{min} = A_N \sigma^n$ | $A_N$ | 3.715E-34 | 6.026E-29 |
| | $n$ | 13.01 | 10.36 |
| Larson-Miller creep model $\sigma = A_{LM} * LMP + B_{LM}$ | $A_{LM}$ | -0.05655 | -0.07858 |
| | $B_{LM}$ | 2005 | 2711 |
| Monkman-Grant creep model $t_f \dot{\varepsilon}_{min}^m = C_{MG}$ | $m$ | 0.6883 | 0.8736 |
| | $C_{MG}$ | 20.18 | 0.8706 |

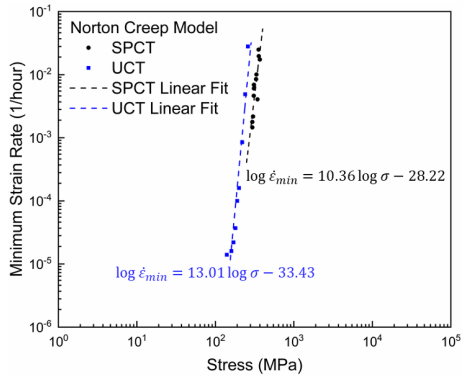


(a)

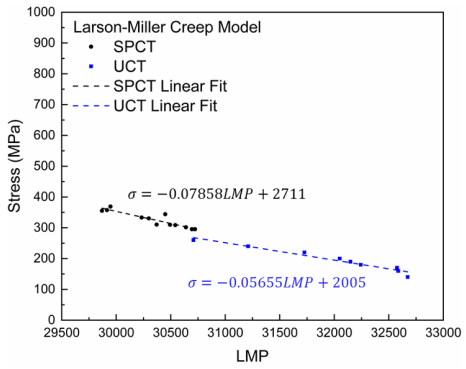


(b)

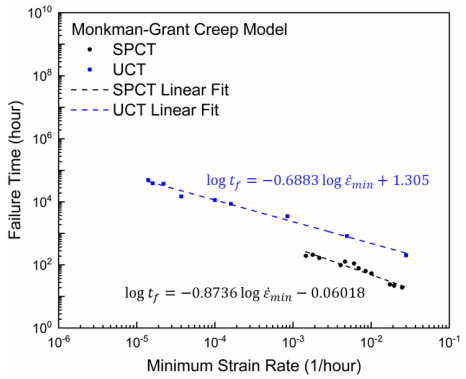


(c)

Fig. 6. Creep properties evaluation models of modified 9Cr-1Mo steel for comparison between small punch and uniaxial creep test: (a) Norton; (b) Larson-Miller; (c) Monkman-Grant.

linear fitting to the test data, so the material constants were the same. However, the Norton and Monkman-Grant models were constructed by directly applying non-linear fitting to the test data (as described in the previous section) and the test data were converted to logarithmic scale and then constructed by applying linear fitting. Due to the difference in the fitting method, there was a slight difference in the material constant results in the Norton and Monkman-Grant models. Nevertheless, it can be seen from Fig. 6 that each of the creep property evaluation models constructed using UCT and SPCT showed consistent tendencies. With the Norton and Larson-Miller models, since the results were quite similar between the two test methods, it was possible to successfully predict the creep properties of the long-term UCT by constructing the models using only the short-term SPCT. With the Monkman-Grant model, however, there was a difference between the UCT and SPCT methods, which we presumed was because the failure time was underestimated compared to the minimum strain rate due to the SPCT methodology in which a very thin specimen is placed in a multi-axial stress state. In the case of the Larson-Miller model, which includes the failure time such as the Monkman-Grant model, because the failure time was not directly used but instead converted to $LMP$ before use, it is judged that a small error occurred between the two test methods compared to the Monkman-Grant model.

## 5. Conclusion

This paper evaluates the creep properties of modified 9Cr-1Mo steel at 550 °C using only SPCT. SPCT was performed under four different loading conditions: 62.5 kgf, 65 kgf, 70 kgf, and 75 kgf, and was repeated three times under each loading condition to ensure the reliability of the test results. During SPCT the average failure times were measured as 190.52 hour, 105.51 hour, 72.02 hour, and 21.79 hour under each loading condition. In order to evaluate the creep properties of metallic materials using SPCT, wherein the displacement and load are derived as outputs, it is necessary to convert these data into the strain and stress of the conventional test method UCT. The displacement of SPCT was converted into the strain of UCT using the equivalent strain formulation proposed by Lee et al. [19], and the load of SPCT was converted into the stress of UCT using the equivalent stress formulation proposed by Kim et al. [20]. Using the data converted from SPCT, the Norton, Larson-Miller, and Monkman-Grant models were constructed to evaluate the creep properties of the modified 9Cr-1Mo steel. Each model was reconstructed using a triangular relationship with common variables among the models. The three models constructed through SPCT and the triangular relationship among them showed very similar results. These results demonstrate that the creep property evaluation models can be successfully constructed using only SPCT. The same creep property evaluation models were constructed using long-term UCT data of modified 9Cr-1Mo steel with creep life between 200 and 50000 hours at the same temperature used by

NIMS [25]. Each of the three models constructed using short-term SPCT and long-term UCT data showed consistent tendencies. In particular, the Norton and Larson-Miller models showed considerable agreement between the two test methods. However, in the Monkman-Grant model, a discrepancy occurred between the two test methods, probably because the failure time was underestimated compared to the minimum strain rate due to the SPCT methodology in which a very thin specimen is placed in a multi-axial stress state.

## Acknowledgments

This research was supported by Basic Science Research Program through the National Research Foundation of Korea (NRF) funded by the Ministry of Education (2021R1A6A1A 03039696).

## Nomenclature

$a$ : Lower die inner radius
$F$ : SPCT load
$h$ : SPCT displacement
$LMP$ : Larson-Miller parameter
$R$ : Punch ball radius
$S_{ij}$ : Deviatoric stress tensor
$t_f$ : Creep life
$T$ : Absolute temperature
$T$ : Specimen thickness
$T_0$ : Specimen initial thickness

### *Greek symbols*

$\alpha$ : Non-dimensional correction factor
$\dot{\varepsilon}_{min}$ : Minimum strain rate
$\varepsilon'_{ij}$ : Deviatoric strain tensor
$\varepsilon_{eq}$ : Equivalent strain
$\varepsilon_{ij}$ : Plastic strain tensor
$\varepsilon_T$ : Radial strain
$\varepsilon_\theta$ : Circumferential strain
$\varepsilon_\varphi$ : Meridional strain
$\mu$ : Friction coefficient
$\sigma$ : UCT stress
$\sigma'_{eq}$ : Equivalent stress including frictional effect
$\sigma_{eq}$ : Equivalent stress
$\sigma_\theta$ : Circumferential stress
$\sigma_\varphi$ : Meridional stress
$\varphi$ : Contact angle between specimen and punch ball

## References

[1] IEA, *World Energy Balances: Overview*, International Energy Agency (2020).
[2] IAEA, *Energy, Electricity and Nuclear Power Estimates for the Period up to 2050*, International Atomic Energy Agency (2019).
[3] L. K. Mansur, A. F. Rowcliffe, R. K. Nanstad, S. J. Zinkle, W. R. Corwin and R. E. Stoller, Materials needs for fusion, generation IV fission reactors and spallation neutron sources - similarities and differences, *Journal of Nuclear Materials*, 329-333 (2004) 166-172.
[4] K. L. Murty and I. Charit, Structural materials for gen-IV nuclear reactors: challenges and opportunities, *Journal of Nuclear Materials*, 383 (2008) 189-195.
[5] I. Charit and K. L. Murty, Structural materials issues for the next generation fission reactors, *JOM*, 62 (9) (2010) 67-74.
[6] ASTM E139-11(2018), *Standard Test Methods for Conducting Creep, Creep-Rupture, and Stress-Rupture Tests of Metallic Materials*, ASTM International, West Conshohocken (2018).
[7] M. P. Manahan, A. S. Argon and O. K. Harling, The development of a miniaturized disk bend test for the determination of postirradiation mechanical properties, *Journal of Nuclear Materials*, 103-104 (1981) 1545-1550.
[8] F. H. Huang, M. L. Hamilton and G. L. Wire, Bend testing for miniature disks, *Nuclear Technology*, 57 (2) (1981) 234-242.
[9] M. Abendroth and M. Kuna, Determination of deformation and failure properties of ductile materials by means of the small punch test and neural networks, *Computational Materials Science*, 28 (2003) 633-644.
[10] E. Altstadt, H. E. Ge, V. Kuksenko, M. Serrano, M. Houska, M. Lasan, M. Bruchhausen, J.-M. Lapetite and Y. Dai, Critical evaluation of the small punch test as a screening procedure for mechanical properties, *Journal of Nuclear Materials*, 472 (2016) 186-195.
[11] B. Ule, T. Sustar, F. Dobes, K. Milcka, V. Bicego, S. Tettamanti, K. Maile, C. Schwarzkopf, M. P. Whelan, R. H. Kozlowski and J. Klaput, Small punch test method assessment for the determination of the residual creep life of service exposed components: outcomes from an interlaboratory exercise, *Nuclear Engineering and Design*, 192 (1999) 1-11.
[12] Z. Yang and Z. Wang, Relationship between strain and central deflection in small punch creep specimens, *Pressure Vessels and Piping*, 80 (2003) 397-404.
[13] K. Milicka and F. Dobes, Small punch testing of P91 steel, *Pressure Vessels and Piping*, 83 (2006) 625-634.
[14] T. Izaki, T. Kobayashi, J. Kusumoto and A. Kanaya, A creep life assessment method for boiler pipes using small punch creep test, *International Journal of Pressure Vessels and Piping*, 86 (2009) 637-642.
[15] T. H. Hyde, M. Stoyanov, W. Sun and C. J. Hyde, On the interpretation of results from small punch creep tests, *The Journal of Strain Analysis for Engineering Design*, 45 (2010) 141-164.
[16] J. Chen, Y. W. Ma and K. B. Yoon, Finite element study for determination of material's creep parameters from small punch test, *Journal of Mechanical Science and Technology*, 24 (6) (2010) 1195-1201.
[17] F. Hou, H. Xu, Y. Wang and L. Zhang, Determination of creep property of 1.25Cr0.5Mo pearlitic steels by small punch test, *Engineering Failure Analysis*, 28 (2013) 215-221.
[18] J. M. Alegre, I. I. Cuesta and M. Lorenzo, An extension of the Monkman-Grant model for the prediction of the creep rupture time using small punch tests, *Experimental Mechanics*, 54

(2014) 1441-1451.
[19] T. Lee, F. A. Ibupoto, J. H. Lee, B. J. Kim and M. K. Kim, A direct methodology for small punch creep test, *Experimental Mechanics*, 56 (2016) 395-405.
[20] J. H. Kim, U. Ro, H. Lee, S. J. Kang, B. H. Lee and M. K. Kim, A direct assessment of creep life based on small punch creep test, *Theoretical and Applied Fracture Mechanics*, 104 (2019) 102346.
[21] J. Chakrabarty, A theory of stretch forming over hemispherical punch heads, *International Journal of Mechanical Sciences*, 12 (4) (1970) 315-325.
[22] F. H. Norton, *The Creep of Steels at High Temperatures*, McGraw-Hill, New York (1929).
[23] F. R. Larson and J. Miller, A time-temperature relationship for rupture and creep stresses, *Transactions of the American Society of Mechanical Engineers*, 74 (1952) 765-775.
[24] F. C. Monkman and N. J. Grant, An empirical relationship between rupture life and minimum creep rate in creep rupture tests, *Proceedings of American Society for Testing Materials International*, 56 (1956) 593-620.
[25] NIMS, *Creep Data Sheet No. 43A*, National Institute for Materials Science (2014).
[26] X. Mao, T. Shoji and H. Takahashi, Characterization of fracture behavior in small punch test by combined recrystallization-etch method and rigid plastic analysis, *Journal of Testing and Evaluation*, 15 (1) (1987) 30-37.
[27] B. J. Kim, N. H. Cho, M. K. Kim and B. S. Lim, Effect of friction coefficient on the small punch creep behavior of AISI 316L stainless steel, *Korean Journal of Metal and Materials*, 49 (7) (2011) 515-521.
[28] T. Shrestha, M. Basirat, I. Charit, G. P. Potirniche, K. K. Rink and U. Sahaym, Creep deformation mechanisms in modified 9Cr-Mo steel, *Journal of Nuclear Materials*, 423 (2012) 110-119.
[29] K. Guguloth and N. Roy, Creep deformation behavior of 9Cr1MoVNb (ASME Grade 91) steel, *Materials Science and Engineering A*, 680 (2017) 388-404.
[30] J. Y. Jeong, J. W. Im and Y. T. Keum, Effects of friction coefficient on creep life assessment of sheet, *Transactions of Materials Processing*, 19 (7) (2010) 435-440.
[31] B. K. Choudhary, W. G. Kim, M. D. Mathew, J. Jang, T. Jayakumar and Y. H. Jeong, On the reliability assessment of creep life for grade 91 steel, *Procedia Engineering*, 86 (2014) 335-341.

**Sangyeop Kim** is a Graduate Student of the School of Mechanical Engineering, Sungkyunkwan University, Korea. He received his B.S. degree in School of Mechanical Engineering from Sungkyunkwan University, Korea, in 2019. His research interests include material property evaluation and computer aided engineering.

**Uijeong Ro** is a Graduate Student of the School of Mechanical Engineering, Sungkyunkwan University, Korea. He received his B.S. degree in School of Mechanical Engineering from Sungkyunkwan University, Korea, in 2018. His research interests include material property evaluation and computer aided engineering.

**Yong Hwi Kim** is a Graduate Student of the School of Mechanical Engineering, Sungkyunkwan University, Korea. He received his B.S. degree in School of Civil Engineering from Ajou University, Korea, in 2017 and M.S. degree in School of Mechanical Engineering from Sungkyunkwan University, Korea, in 2020. His research interests include structure analysis and metal AM.

**Taeksang Lee** is an Assistant Professor of the Department of Mechanical Engineering, Myongji University, Korea. He received his B.S. and M.S. degrees in School of Mechanical Engineering from Sungkyunkwan University, Korea, in 2014 and 2016, respectively, and Ph.D. degree from Purdue University in 2020. His research interests include computational biomechanics based on data-driven modeling, finite element method, and Bayesian inference.

**Moon Ki Kim** is a Professor of the School of Mechanical Engineering, Sungkyunkwan University, Korea. He received his B.S. and M.S. degrees in School of Mechanical Engineering from Seoul National University in 1997 and 1999, respectively, and Ph.D. degree from Johns Hopkins University in 2004. He had been an Assistant Professor in the Department of Mechanical and Industrial Engineering at University of Massachusetts, Amherst from 2004 to 2008. His research interests include computational structural biology based on robot kinematics, bioinstrumentations and multiscale modeling and simulation.